Consideration of the Interactions Between the Reaction Zones in the New Extended Eddy Dissipation Concept model

N. Romero-Anton[a], K. Martin-Escudero[a], Mengmeng Ren[b], Z. Azkorra-Larrinaga[a]

[a]*ENEDI Research Group, Faculty of Engineering in Bilbao, University of the Basque Country UPV/EHU, Plaza Torres Quevedo 1, 48013, Bilbao, Spain*

[b]*School of Metallurgical Engineering, Xi'an University of Architecture and Technology, Xi'an 710055, China*

E-mail address: naiara.romero@ehu.eus

Abstract

The latest Direct Numerical Simulation (DNS) modelling results in flameless combustion suggest interactions between the combustion reaction zones. The New Extended Eddy Dissipation Concept (NE-EDC) model, where model coefficients are calculated based on local Reynolds and Damköhler numbers, was proposed to improve the standard Eddy Dissipation Concept (EDC) model's accuracy when modelling flameless combustion, but this model does not include the interactions between the reaction zones.

In this work, a revised version of the NE-EDC model is presented, called here Generalized NE-EDC model, where the chemical time scale is calculated in detail, considering the reaction rates of CH_4, H_2, O_2, CO and CO_2, making the interaction between the reaction zones more realistic (in the NE-EDC only a one-step CH_4 global reaction mechanism is considered). A comparative study of four global reaction mechanisms is carried out to select the best mechanism for chemical time scale definition: the adjusted Jones & Lindstedt (JL1); the adjusted Westbrook & Dryer (WD1); the adjusted Westbrook & Dryer (WD2); and the one-step CH_4 global mechanism (1-step).

The four global reaction mechanisms, in combination with the NE-EDC model, are applied to the Delft lab-scale furnace and the modelling results are compared against those experimental measurements. The NE-EDC modelling results, in combination with WD2, present a slight improvement over the other global mechanisms in flameless modelling.

Key words: Flameless combustion, MILD combustion, chemical time scale, reaction zones, Eddy Dissipation Concept, CFD.

Highlights

- The Generalized NE-EDC is developed to consider interactions between reaction zones
- The interaction is considered using a detailed chemical time scale (τ_c) calculation
- A comparative study of 4 global reaction mechanisms is made for the τ_c definition
- The WD2 global mechanism brings a slight improvement compared to the 1-step CH_4

Nomenclature

A_{fj}		pre-exponential constant of Arrhenius' law
C_{D1}	[-]	model parameter in the EDC model
C_{D2}	[-]	model parameter in the EDC model
C_{ξ}	[-]	finite structure constant in the EDC model
C_{τ}	[-]	residence time constant in the EDC model
D_a	[-]	Damköhler number
E_j	[kJ/kmol]	activation energy
k	[m^2/s^2]	turbulent kinetic energy
K_{fj}		forward rate of reaction j
K_{rj}		backward rate of reaction j
L^*	[m]	fine structure length scale in the EDC model
M_k	[-]	species k symbol
$R_{i,r}$	[kg/(s·m^3)]	net rate of production of species due to reaction r
R_{kj}	[kmol/m^3/s]	net molar production rate of each species k in reactions j [kmol/m^3/s]:
S_L	[m/s]	laminar flame speed (burning velocity)
t'_{kj}	[-]	experimental concentration exponent
t''_{kj}	[-]	experimental concentration exponent
$\widetilde{U}$	[m/s]	mean axial velocity
W_k	[kg/kmol]	molecular weight of species k:
$[X_k]$	[kmol/m^3]	molar concentration
Y_k	[-]	mass fraction of species k
Y_i	[-]	mean mass fraction in computational cell
Y_i^*	[-]	species mass fraction in the EDC fine structure

Greek symbols

β_j	[-]	temperature exponent constant of Arrhenius' law
ε	[J/(kg·s)]	turbulent energy dissipation rate
η_k	[m]	Kolmogorov length scale

v	[m^2/s]	laminar kinematic viscosity
v'_{kj}	[-]	reactants' molar stoichiometric coefficient of species k in reaction j.
v''_{kj}	[-]	products' molar stoichiometric coefficient of species k in reaction j.
ξ^*	[-]	(normalized) fine structure length in the EDC model
$\bar{\rho}$	[kg/m^3]	mean density
τ_c	[s]	chemical time scale
τ_c^*	[s]	chemical time scale of fine structure in the EDC model
τ^*	[s]	residence time scale in the EDC model
ω'_j	[kmol/m^3/s]	progress rate of reaction for the reaction pair
ω_k	[kg/m^3/s]	reaction rate of species k

Abbreviations

EDC	Eddy Dissipation Concept model
E-EDC	Extended Eddy Dissipation Concept
DNS	Direct Numerical Simulation
JHC	Jet-in-Hot-Coflow
JL	Jones and Lindstedt
MILD	Moderate or Intense Low Oxygen Dilution
NE-EDC	New Extended Eddy Dissipation Concept
NP	Norbert Peters
PFR	Plug Flow Reactor
PW	Peters and Williams
RANS	Reynolds-Averaged Navier–Stokes
UDF	User Define Functions
UDM	User Define Memory
WD	Westbrook and Dryer

1 Introduction

Climate change is the biggest challenge that society has to deal with, and the burning of fossil fuels to release energy is the main cause of the greenhouse effect [1]. Flameless combustion, also known as moderate or intense low oxygen dilution (MILD) combustion, is a climate-friendly combustion technology able to reduce pollutant emissions (NO_x) and improve energy efficiency [2].

In order to gain an in-depth understanding of flameless combustion, research has been conducted in Jet-in-hot co-flow (JHC) burners [3]-[4], as well as in enclosed lab-scale furnaces [5]-[6]. With the data from these experimental set-ups, flameless Reynolds Average Navier Stoke (RANS) modelling studies have been validated. The first conclusion suggests that the temperature gradient in the mean profile is lower than in conventional combustion. Thus, the chemical time scale can be longer, thickening reaction zones. Therefore, standard turbulence-chemistry interaction models, such as the Eddy Dissipation Concept (EDC) and flamelet based model, may not be accurate for flameless combustion modelling, as they do not consider this feature. The EDC model, for example, calculates the reaction rate based on two constants empirically chosen for conventional combustion ($C_\xi = 2.1377$ and $C_\tau = 0.4082$), so they do not take into account the dilution effect of flameless combustion. The Flamelet Generation Manifold (FGM) model, for example, generates flamelet tables based on pure fuel and pure air as boundary conditions, without taking into consideration diluted reactants [7]-[8]. Therefore, new models or extensions of the existing models should be developed to model flameless combustion.

The EDC model has been widely used for flameless modelling and the first approach to improve its accuracy was to change the model's constants value (C_ξ and C_τ), in an arbitrary way, calibrating them with experimental data [9]-[10]. Later, an extension of the EDC model was proposed, the Extended EDC (called here E-EDC), where the model's coefficients are calculated based on local Reynolds and Damköhler numbers, so that the calibration of the model coefficients is avoided [11]. To better model flameless combustion, then, the New Extended EDC (NE-EDC) model was developed [12]. This model follows a similar strategy to the E-EDC model, that is, model constants are also calculated based on local Reynolds and Damköhler numbers. Nevertheless, the NE-EDC model postulates the fine structure length scale is equal to the Kolmogorov scale $L^* = \eta_k$ (for

more details of this assumption goes to reference [12]); while the E-EDC model does not follow this assumption. Additionally, the NE-EDC model proposed laminar flame speed calculation as $L^* = \tau_c^* * S_L$ and the proportionality factor for laminar flame speed calculation used in the E-EDC model is omitted. These EDC model extensions show a better consistency with experimental data than the standard EDC model in flameless combustion modelling [12]. Note that both the E-EDC and the NE-EDC present important advantages, as model coefficients are calculated during modelling and calibration with experimental data is not necessary. Of these, the NE-EDC model seems to provide better radial profiles of the mean temperature on a lab-scale furnace application [12]. Recently, Lewandowski and Ertesvåg [13] and Ertesvåg [14] carried out a review of the proposed changes, commented above, to the standard EDC model for flameless modelling with respect to the original ideas of the EDC model proposed by Magnussen et al. [15]-[16].

To better understand reaction zone behaviour under flameless combustion, Direct Numerical Simulation (DNS) modelling has been carried out [17]-[19]. The DNS modelling results suggested interactions between the combustion reaction zones, so this feature can invalidate the commonly used combustion assumption: infinity fast-chemistry and flamelet modelling [20]. Under this circumstance, a Generalized E-EDC model has been proposed [21]-[23], based on the model developed by Parente et al. [11], but including detailed chemical kinetics for considering reaction zone interaction. In the Generalized E-EDC work, the global reaction mechanisms and Arrhenius constant values used are not specified. Driscoll et al. [24] recently discussed the necessary conditions for distributed reactions, still leaving possibilities for the EDC model to be applied in MILD combustion [25]. In the Generalized E-EDC, the chemical time scale is calculated considering the reaction rates of CH_4, H_2, O_2, CO and CO_2, but not following the CH_4 one-step mechanism (as was done in the E-EDC). Additionally, the Generalized E-EDC eliminates the proportionality factor in laminar flame velocity following the NE-EDC suggestion [11]. The Generalized E-EDC model presents a better consistency with experimental data in a JHC furnace than the E-EDC.

In consideration of the recent DNS modelling findings that suggest interactions between the reaction zones, for the first time, this work presents the Generalized NE-EDC model. It is a revised version of the NE-EDC model [12] and, in order to include the DNS modelling findings (the interaction between the reaction zones), the chemical time scale is calculated considering the

reaction rates of CH_4, H_2, O_2, CO and CO_2 by a simple generalized method. In the original NE-EDC model, the chemical time scale was calculated following the CH_4 1-step global mechanism [12]. Therefore, in this work, a new and detailed chemical time scale calculation methodology is implemented in the NE-EDC model to improve the flameless combustion model, making it more realistic.

The new chemical time scale is selected in this work by a comparative study of four global reaction mechanisms (note that a detailed mechanism is used to calculate temperature and species concentrations during modelling): the Jones & Lindstedt adjusted global mechanism (JL1), where the 4th mechanism of the standard 4-step global mechanism of JL is adjusted to flameless combustion; the Westbrook & Dryer adjusted global mechanism (WD1), which includes the H_2 oxidation rate for flameless application; the Westbrook & Dryer adjusted global mechanism (WD2), which differs from the WD1 in the CO oxidation rate consideration; and finally, the one-step CH_4 global mechanism. These global reaction mechanisms are selected as they provided the best results in the works [26]-[27]. In this work the calculation of the chemical time scale is carried out where the calculation methodology is explained for the first time in detail. It is implemented in ANSYS Fluent by User Define Functions (UDF) and User Define Memory (UDM). Additionally, the Generalized NE-EDC model is applied in an enclosed lab-scale furnace, a Delft lab-scale furnace, and the modelling results are compared against those experimental measurements.

Fig. 1 summarizes the general approach of this study, with the investigations that have been carried out to date and those carried out for the first time in this work.

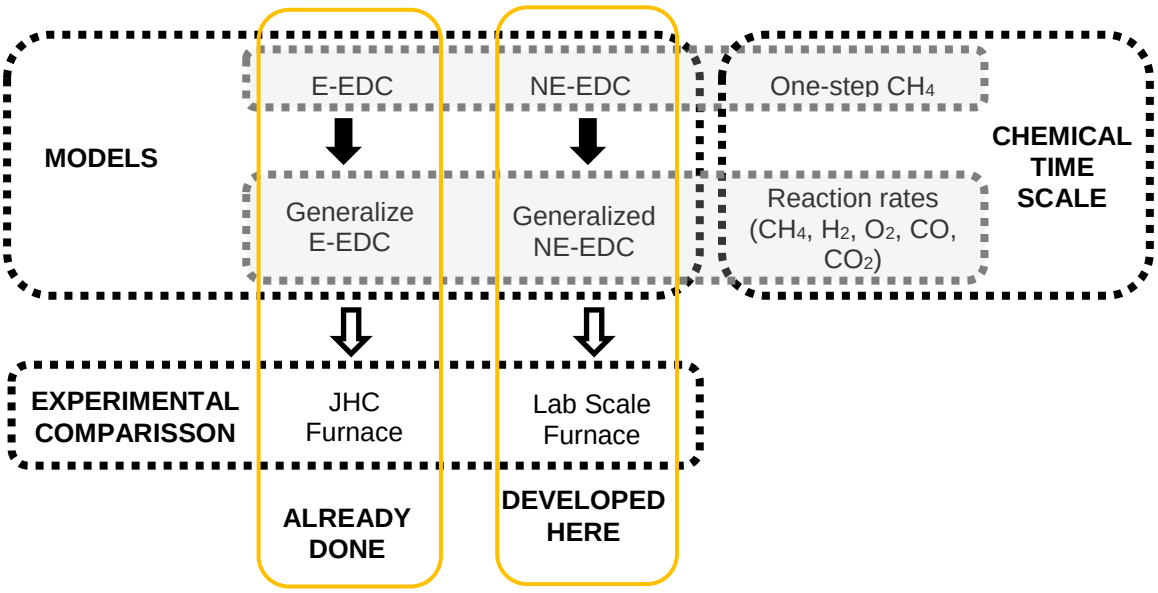

Fig. 1 *Summary of the extended EDC models situation*

2 Model description

The EDC model's main idea is that chemical reactions in turbulent flow occur fast and in small eddies (fine structures denoted by the superscript *) treated as a reactor [16]. Then, a cascade model links the fine structures to the mean turbulence field resolved by RANS, so the EDC consists of a cascade model and a reactor model. This simplification makes the EDC model flexible and applicable to several flame structures. ANSYS Fluent's EDC model uses a Plug Flow Reactor (PFR), assuming that the fine structure reacts within an interval of time with no mixing [28].

The reaction rate of the EDC is obtained by the mass balance of the fine-structure reactor and the mean reaction rate of each mean species mass fraction is finally given by:

$$R_{i,r} = \frac{\bar{\rho}(\xi^*)^2}{\tau^*[1-(\xi^*)^3]}(Y_i^* - Y_i) \tag{1}$$

where ξ^* is a fine structure length scale (based on the ratio of the mass of regions containing fine structures and the total mass), τ^* is the fine structure residence time (based on the mass transfer rate between the fine structures and the surrounding), $\bar{\rho}$ is the mean density and Y_i is species mass fraction. The EDC model derivation, based on the energy cascade concept, assumes that all energy is transferred from large-scale eddies to small eddies, describing the fine structure length ξ^* and the residence time scale τ^*as:

$$\xi^* = \left(\frac{3C_{D2}}{4C_{D1}^2}\right)^{1/4}\left(\frac{v\varepsilon}{k^2}\right)^{1/4} = C_\xi\left(\frac{v\varepsilon}{k^2}\right)^{1/4} \tag{2}$$

$$\tau^* = \left(\frac{C_{D2}}{3}\right)^{1/2}\left(\frac{v}{\varepsilon}\right)^{1/2} = C_\tau\left(\frac{v}{\varepsilon}\right)^{1/2} \tag{3}$$

where v is the kinetic viscosity, ε the dissipation rate, k the turbulent kinetic energy, C_{D2} and C_{D1} the EDC model's coefficients, C_ξ the finite structure constant and C_τ the residence time constant. The standard EDC model developed by Magnussen and co-workers [15]-[16] gives an empirical value for $C_\xi = 2.1377$ and $C_\tau = 0.4083$ based on conventional combustion. However, the NE-

EDC model calculates these constant values based on the local Reynolds and Damköhler numbers following energy-cascade concepts (for more details go to Romero-Anton et al. [12]):

$$C_\tau = \left(\frac{C_{D2}}{3}\right)^{1/2} = \frac{1}{2}\frac{1}{\sqrt{(Re_T + 1)}Da^*} \quad (4)$$

$$C_\xi = \left(\frac{3C_{D2}}{4C_{D1}^2}\right)^{1/4} = \sqrt{\frac{3}{2}(Re_T + 1)}Da^{*3/4} \quad (5)$$

In this work, these two equations are used, limiting coefficient values between 0.2< C_τ <0.4083 and 2.1377 <C_ξ <13, always between the limits accepted in Ref. [14]. Values outside this range mean fast chemistry, while in flameless combustion it is known to have a Da number around unity [29].

In the NE-EDC model [12], a one-step global reaction rate of CH_4 is considered for chemical time scale calculation, $\tau_c = \frac{1}{8.3\ 10^5 exp\left(-\frac{T_A}{T}\right)}$, where $T_A = 15{,}100\ K$. The chemical time scale is calculated by UDF and then, in combination with the flow time scale calculated by ANSYS Fluent, the UDF calculates the local Da number. Later, the Da number value is applied in both Eq. (4) and Eq. (5), and the EDC model constants are calculated.

In order to include the interaction between the reaction zones suggested by the DNS results, it would be interesting to study the impact of calculating the chemical time scale considering the reaction rate of other species of minor concentration. Accordingly, in this work, the Generalized NE-EDC is proposed in order to also consider the CH_4, H_2, O_2, CO_2 and CO species reaction rates in the chemical time scale calculation.

2.1 Global reaction mechanisms

So as not to increase modelling computational time, global reaction mechanisms are proposed to calculate the chemical time scale.

Accurate and widely applied global mechanisms for CH_4 combustion are; the Jones-Lindstedt (JL) mechanism [30], the Westbrook-Dryer mechanism (WD) [31], the Norbert-Peters 4 step mechanism (NP) [32] and the Peters-Williams 3 (PW) step mechanism [33]. It should be mentioned that these models were developed and applied in conventional combustion.

The NP and PW global mechanisms were developed for conventional combustion, so their Arrhenius coefficients are defined for that application. Nevertheless, the JL and WD mechanisms have been applied and adjusted for flameless combustion. Kim [26] and Wang [27] applied the JL and WD global mechanisms in flameless combustion and they developed new Arrhenius constant values for flameless application. In their work, the adjusted global mechanism of JL (JL1) and two adjusted global mechanisms of WD (WD1 and WD2) show a better consistency with flameless combustion experimental data. Thus, in this work, these three global reaction mechanisms are implemented on the NE-EDC model by UDF and they are modelled in a Delft lab-scale furnace. Note that the global reaction mechanisms are used only to compute the chemical time scale through UDF while a detailed mechanism with 16 species [34] is used to calculate temperature and species concentrations during modelling.

- **Jones & Lindstedt adjusted global mechanism (JL1)**

This mechanism is based on the standard 4-step global mechanism of JL [30]. In flameless combustion O_2 concentration is reduced, so the O_2 partial pressure is lower. Under this situation, the fuel oxidation rate become slower. Thus, the 4th mechanism of the standard 4-step global mechanism of JL is adjusted to this combustion system, following the suggestions of Marinov et al. [35] and Wang et al. [27]:

{C1} $CH_4 + 0.5O_2 \rightarrow CO + 2H_2$

{C2} $CH_4 + H_2O \rightarrow CO + 3H_2$

{C3} $CO + H_2O \leftrightarrow CO_2 + H_2$

{C4} $H_2 + 0.5O_2 \leftrightarrow H_2O$

- **Westbrook & Dryer adjusted global mechanism (WD1)**

Westbrook and Dryer [31] developed a 2-step global reaction mechanism. In the adjusted WD1 release, the CH_4 and CO oxidation rates are not changed to the original mechanism, but the H_2 oxidation rate is added (C4), as happens in JL1:

{C5} $CH_4 + 1.5O_2 \rightarrow CO + 2H_2O$

{C6} $CO + 0.5O_2 \leftrightarrow CO_2$

{C4} $H_2 + 0.5O_2 \leftrightarrow H_2O$

- **Westbrook & Dryer adjusted global mechanism (WD2)**

This mechanism maintains the CH_4 and H_2 oxidation rates as WD1, but changes the CO oxidation rate. This change is made considering the CO dependency on the pressure equilibrium of $[CO]/[CO_2]$, following Andersen et al. [36]:

{C5} $CH_4 + 1.5O_2 \rightarrow CO + 2H_2O$

{C7} $CO + 0.5O_2 \leftrightarrow CO_2$

{C4} $H_2 + 0.5O_2 \leftrightarrow H_2O$

Table 1 summarizes the Arrhenius parameters defined for each global reaction mechanism:

Table 1 *Global mechanism's Arrhenius coefficient values and reaction orders*

Nº	A	β	E_a/R	Reaction orders	Ref
C1	$4.4*10^{11}$	0	15095	$[CH_4]^{0.5}[H_2O]$	JL [30]
C2	$3.0*10^{8}$	0	15095	$[CH_4][O]$	JL [30]
$C3_f$	$2.75*10^{9}$	0	10065	$[CO][H_2O]$	JL [30]
$C3_b$	$6.71*10^{10}$	0	13688	$[CO_2][H_2]$	Wang et al. [27]
$C4_f$	$7.91*10^{10}$	0	17609	$[H_2][O_2]^{0.5}$	Marinov et al. [35]
$C4_b$	$3.48*10^{13}$	0	47907	$[H_2O]$	Wang et al. [27]
C5	$5.03*10^{11}$	0	24056	$[CH_4]^{0.7}[O]^{0.8}$	WD [31]
$C6_f$	$2.24*10^{12}$	0	20484	$[CO][O2]^{0.25}[H2O]^{0.5}$	WD [31]
$C6_b$	$5*10^{8}$	0	20484	$[CO_2]$	WD [31]
$C7_f$	$2.24*10^{6}$	0	5032	$[CO][O2]^{0.25}[H2O]^{0.5}$	Andersen et al. [36]

$C7_b$	$1.10*10^{13}$	-0.97	39452	$[CO][O2]^{-0.25}[H2O]^{0.5}$	Andersen et al. [36]

Units in kmol, m^3, K, s, kJ.

2.2 Implementation Methodology

The global reaction mechanisms described in section 2.1 have been implemented in ANSYS Fluent by UDF and UDM. The UDF is a tool available in ANSYS Fluent to enhance the standard characteristics of the programme. The user is responsible for creating, debugging and validating them and, using an interface available in ANSYS Fluent, they are called by demand or hooked. The code needs to be compiled or interpreted when it is loaded in ANSYS Fluent and, for this work, the Microsoft Visual Studio compiler has been used.

Considering the chemical kinetics of a system of N species reacting through M reactions, we get:

$$\sum_{k=1}^{N} v'_{kj}\, M_k \;\leftrightarrow\; \sum_{k=1}^{N} v''_{kj}\, M_k \quad \text{for} \;\; j = 1, M \tag{6}$$

where M_k is the species k symbol and v'_{kj} & v''_{kj} are the molar stoichiometric coefficients of species k in reaction j. It should be mentioned here that reactions could proceed in one direction → (forward, f) or in both directions ↔ (forward, f, and backward, b). Considering the mass conservation, the progress rate of reaction for the reaction pair is defined as [kmol/m^3/s]:

$$\omega'_j = K_{fj} \prod_{k=1}^{N} [X_k]^{v'_{kj}} - K_{rj} \prod_{k=1}^{N} [X_k]^{v''_{kj}} \tag{7}$$

where K_{fj} and K_{rj} are the forward and backward rates of reaction j. In this work, they are calculated by the Arrhenius law:

$$K_{fj} = A_{fj} T^{\beta_j} exp\left(-\frac{E_j}{RT}\right) = A_{fj} T^{\beta_j} exp\left(-\frac{T_{aj}}{T}\right) \tag{8}$$

where A_{fj} is a pre-exponential constant, β_j the temperature exponent constant and E_j the activation energy. The constant values used in this work are defined in Table 1.The backwards rates K_{rj} are calculated considering the equilibrium constant [37].

The progress rate of reaction, (Eq. (7)) is theoretically defined with the stoichiometric coefficients defined by the mass conservation law (v''_{kj} & v'_{kj}). In practice, instead of using stoichiometric coefficients as the concentration exponent, other parameters (t'_{kj}& t''_{kj}) are used. These parameters are calculated based on experimental or detailed chemical numerical modelling. In this work, the exponents of Table 1 are used (t'_{kj}& t''_{kj}).

Once the reaction rate of each species k is calculated (Eq. (7), Eq. (8) and Table 1), the next step is to calculate the net molar production rate of each species k in reactions j [kmol/m^3/s]:

$$R_{kj} = (\Gamma_j(v''_{kj} - v'_{kj})K_{fj}\prod_{k=1}^{N}[X_k]^{t'_{kj}} - K_{rj}\prod_{k=1}^{N}[X_k]^{t''_{kj}}) \quad (9)$$

where $[X_k]$ is the k species molar concentration. Then each k species net mass reaction rate is calculated, multiplying by each species molecular weight W_k:

$$\omega_k = W_k\, R_{kj} \quad (10)$$

Finally, the chemical time scale is calculated

$$\tau_c = \max[Y_k/(\omega_k/\rho)] \quad (11)$$

where ω_k is the reaction rate in [kg/m^3/s] of each species (CH_4, H_2, O_2, CO and CO_2). The reaction rate below ω_k< 10-16 in kg/m^3/s is excluded from the modelling.

Following this methodology, more species are considered for chemical time scale calculation. The UDF calculates the chemical time scale following the described methodology in combination with the flow time scale calculated by ANSYS Fluent. Later, the UDF calculates the Damköhler number, which is replaced in Eq. (4) and Eq. (5). However, this method maintains the efficiency of the NE-EDC model, as it does not require the computational time of the method which calculates the eigenvalues of the Jacobian [38]-[39]. In this work, as the CH_4, H_2, O_2, CO and CO_2 species are considered, the reactions defined in section 2.1 are applied.

This methodology is followed for the global reaction mechanisms described in this work; the JL1, WD1, WD2 and CH_4 one-step global reaction mechanisms. Therefore, four CFD modellings are

developed in this work in a Delft lab-scale furnace. Comparing their modelling results with experimental data, the best global reactions mechanism is selected.

For a better understanding of the methodology, an example is shown for the JL1 global mechanism. First, the progress rates of reaction ω_j' are calculated [kmol/m^3/s]:

$$\omega'_{C1} = 4.4 \cdot 10^{11} exp(\frac{-15095}{T[K]}) \cdot [CH_4]^{0.5}[O_2]^{1.25} \quad (12)$$

$$\omega'_{C2} = 3.0 \cdot 10^{8} exp(\frac{-15095}{T[K]}) \cdot [CH_4][H_2O] \quad (13)$$

$$\omega'_{C3_f} = 2.75 \cdot 10^{9} exp(\frac{-10065}{T[K]}) \cdot [CO][H_2O] \quad (14)$$

$$\omega'_{C3_b} = 6.71 \cdot 10^{10} exp(\frac{-13688}{T[K]}) \cdot [CO_2][H_2] \quad (15)$$

$$\omega'_{C4_f} = 7.91 \cdot 10^{10} \exp(\frac{-17609}{T[K]}) \cdot [H_2][O_2]^{0.5} \quad (16)$$

$$\omega'_{C4_b} = 3.48 \cdot 10^{13} \exp(\frac{-47907}{T[K]}) \cdot [H_2O] \quad (17)$$

Then, the net molar production rates of each species k in reactions j [kmol/m^3/s] are calculated by Eq. (9):

$$\begin{bmatrix} R_{\mathrm{CH_4}} \\ R_{\mathrm{H_2O}} \\ R_{\mathrm{O_2}} \\ R_{\mathrm{CO}} \\ R_{\mathrm{CO_2}} \\ R_{\mathrm{H_2}} \end{bmatrix} = \begin{bmatrix} -1 & -1 & 0 & 0 & 0 & 0 \\ 2 & 2 & -1 & 1 & 1 & -1 \\ -1/2 & 0 & 0 & 0 & -1/2 & 1/2 \\ 1 & 1 & -1 & 1 & 0 & 0 \\ 0 & 0 & 1 & -1 & 0 & 0 \\ 0 & 0 & 1 & -1 & -1 & 1 \end{bmatrix} \cdot \begin{bmatrix} \omega'_{C1} \\ \omega'_{C2} \\ \omega'_{C3_f} \\ \omega'_{C3_b} \\ \omega'_{C4_f} \\ \omega'_{C4_b} \end{bmatrix} \quad (18)$$

The parameters of the matrix represent the difference between the product and reactant stoichiometric coefficients for species k in reactions j. Next, Eq. (10) is applied and the maximum chemical time scale is calculated.

3 Numerical setup

The models are applied to the Delft lab-scale furnace as experimental data is available [41]. Inside the furnace, there is flameless combustion thanks to the recuperative burner injecting natural gas by a single nozzle and preheated air by four separate nozzles (see Fig. 2).

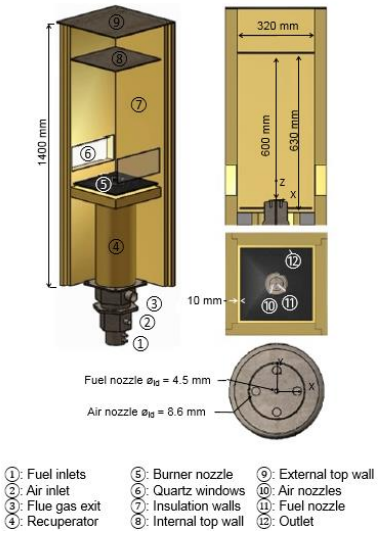

Fig. 2 *Delft lab-scale furnace [41]*

The furnace was operating with Dutch natural gas (mole fractions: CH_4 81.3%, C_2H_6 3.7%, N_2 14.4% and the rest 6%), an equivalence ratio of 0.8, a thermal power of 9kW and fuel and air inlet temperatures of 446K and 886K, respectively, when experimental data for the database were taken. Coherent Anti-stokes Raman Spectroscopy (CARS) made temperature measurements at different heights inside the furnace, as well as Laser Doppler Anemometry (LDA) measured radial profiles of the mean axial velocity ($\widetilde{U}_Z$) at different axial locations. Details of the accuracy of the LDA and CARS measurement techniques are displayed in table 2 of reference [12].

The ANSYS Fluent CFD package was used for a 3-dimension steady-state RANS modelling. As shown in Fig. 3, the modelled computational domain is half of the furnace with about a mesh size of 800,000 cells.

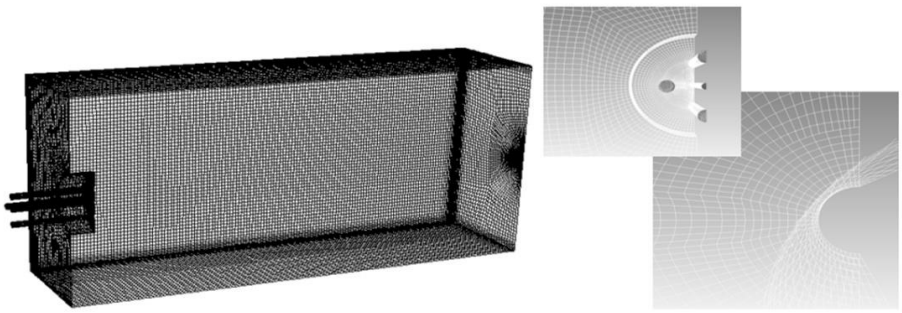

Fig. 3 *computational domain*

The models considered during modelling are the NE-EDC turbulence-chemistry interaction model in combination with four global mechanisms for chemical time scale calculation, the realizable 2-equation $k-\varepsilon$ turbulence model, the Discrete Ordinates (DO) method and the weighted-sum-of-grey-gases model (WSGGM) for the absorption coefficient. The chemical mechanism is the Smooke [34], having 16 species and 25 reactions.

The boundary conditions are defined based on experimental data (see Fig. 4), and are summarized in Table 2. For example, the air inlet is defined as preheated air 846K and mass flow type with a composition of %21 O_2 and 79% N_2 mole fractions. The fuel inlet is Dutch natural gas with a composition of CH_4 81.3%, C_2H_6 3.7%, N_2 14.4% and Ar 6% (in mole fractions) defined as mass flow type. The outlet in this furnace is in the same plane as the input stream and it is defined as pressure outlet type.

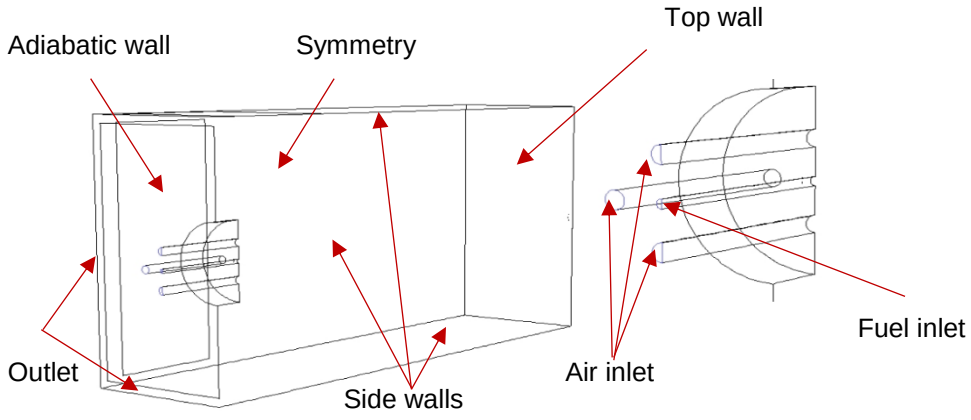

Fig. 4 *Geometry and boundary conditions of the Delft lab-scale furnace*

The thermal boundary conditions of the walls are divided into three. First, the bottom wall of the furnace, which is on the same plane as the inlet streams, is defined as an adiabatic wall with a

heat flux equal to 0 W/m^2. Second, the side walls of the furnace are defined as a wall type boundary with a specified vertical temperature profile obtained through the interpolation of the measured data. Finally, the top wall of the furnace is defined as a wall type boundary, but with a constant temperature equal to the measured value on that wall.

Table 2 *Boundary conditions for simulations*

Name	Type	Value
Air inlet	mass flow type	$\dot{m_{full}} = 9{,}67 * 10\text{^} - 4$ kg/s $\dot{m_{half}} = 4{,}84 * 10\text{^} - 4$ kg/s T= 846 K
Fuel inlet	mass flow type	$\dot{m_{half}}$ =0.000118 kg/s T= 446 K
Outlet	pressure outlet	-
Side Wall	wall type	T: piecewise linear $T(z) = \begin{Bmatrix} 300z + 1150 & 0 < z < 0.3\ [m] \\ 400z + 1120 & 0.3 < z < 0.4\ \ [m] \\ 1280 \end{Bmatrix} K$
Top wall	wall type	T= 1280 K
Bottom wall	wall type	Heat flux 0 W/m^2

Modelling aspects are the same as those used previously by Romero-Anton et al. [12], except for the adjusted global mechanisms for chemical time scale calculation, which implies changes in the Damköhler number and, consequently, in the NE-EDC turbulence-chemistry interaction model constant's value.

4 Results

In this section, a comparison is made between the measured and predicted mean axial velocity and the mean temperatures for each adjusted global mechanism model. Fig. 5 shows the results of the mean axial velocity for the NE-EDC model in combination with the Jones & Lindstedt adjusted global mechanism (JL1), the Westbrook & Dryer adjusted global mechanism (WD1), the

Westbrook & Dryer adjusted global mechanism (WD2) and the one-step CH_4 global mechanism. Experimental data at different axial locations of the furnace (z=3 mm, z=100 mm, z=300 mm and z=500 mm) are also displayed.

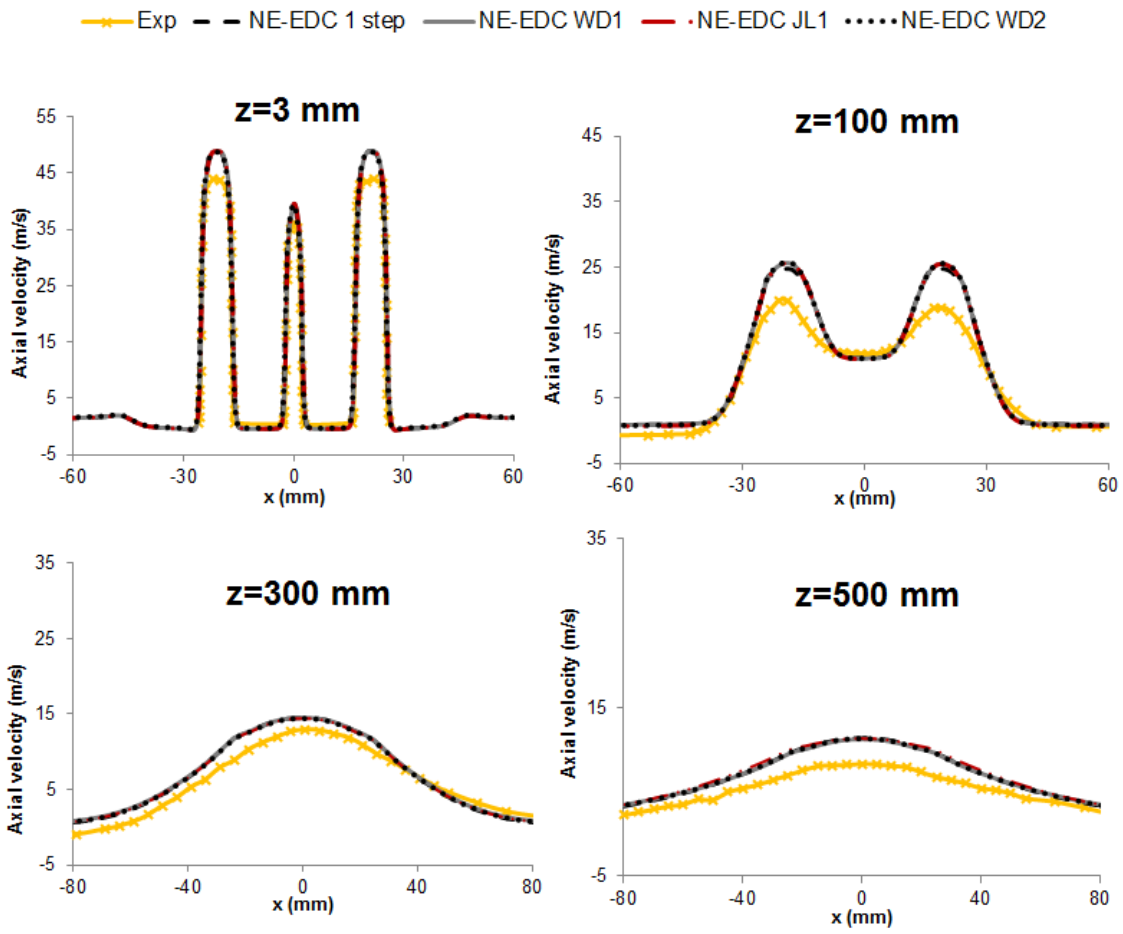

Fig. 5 *Comparison between measured and predicted radial profiles of mean axial velocity*

There is no difference in the mean axial velocity prediction among the four global reaction mechanisms. This is because the same turbulence-chemistry interaction model, realizable $k-\varepsilon$, is used. Finally, this $k-\varepsilon$ model is the cause of the velocity prediction, so it can be said that this turbulence model is appropriate for this study case.

Then, the mean temperature contour of the JL1, the WD1, the WD2 and the 1-step CH_4 global mechanisms are shown (Fig. 6).

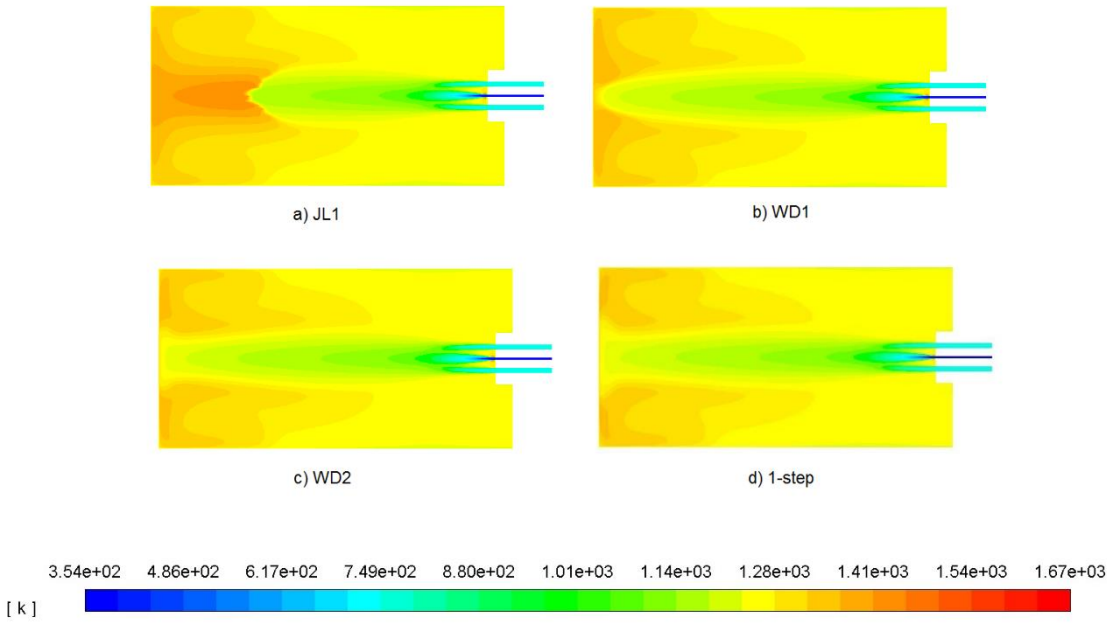

Fig. 6 *Mean temperature contour for JL1, WD1, WD2 and 1-steb global mechanisms*

At first sight, it can be appreciated that the JL1 global mechanism presents greater mean temperature values than the other models, being the only one that exceeds 1400 K in the points away from the flame, while the other global mechanism models provide similar values. For a better viewing, the radial profiles of the mean temperatures are compared in Fig. 7. In this sense, the NE-EDC model, in combination with the JL1, the WD1, the WD2, the 1-step CH_4 global mechanism and experimental data are displayed at different axial locations of the furnace (z=25 mm, z=100 mm, z=200 mm, z=300 mm, z=400 mm and z=500 mm).

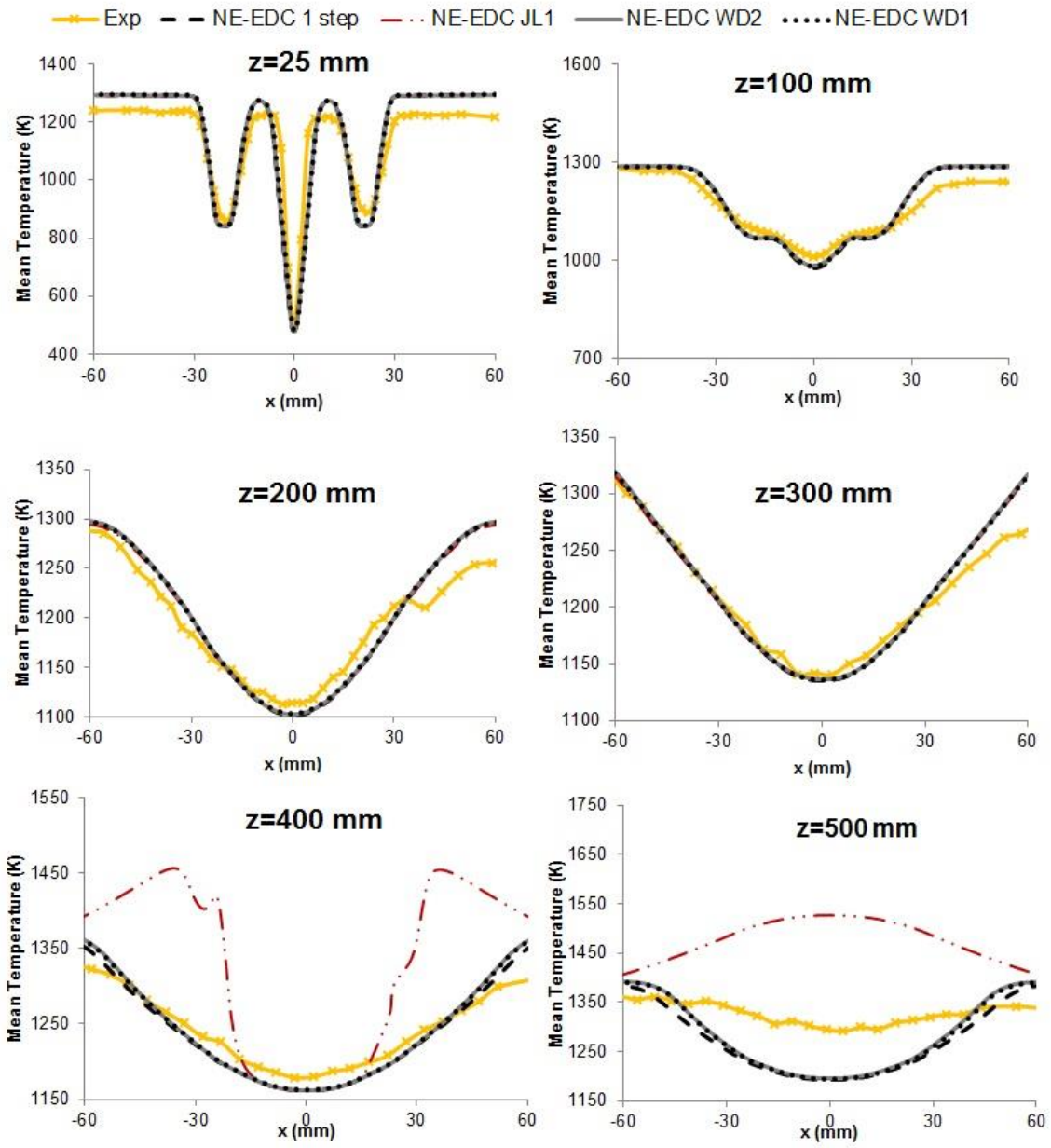

Fig. 7 *Comparison of mean temperature from experimental measurements and from simulations with different global mechanisms*

The results of the four global mechanism models showed good agreement with experimental data and a good match between them in the mean temperature predictions at the nozzle exit (z=25 mm) and at the mid-height of the furnace (z=100, z=200 and z=300 mm). At greater heights (z=400 and z=500 mm), deviance between the four modellings can be appreciated. This is because, according to experimental data, the reaction rate influence on the mean temperature profile starts at a height of 200 mm; upstream, the mixture is preheated and diluted by the recirculation of flue gases [41]. The JL1 model, close to the top wall of the furnace, overpredicts

the mean temperature moving away from experimental data. This deviance is stressed at z=500 mm, where the gradient is the opposite to the experimental data. This feature can also be appreciated in Fig. 6, where a high temperature is displayed close to the furnace top wall. Thus, the JL1 global mechanism is discarded for this flameless combustion furnace modelling.

Among the WD1, WD2 and 1-step global mechanisms, a slight difference can be appreciated at heights of z=400 and z=500 mm because, at this height, autoignition happens constantly. For a better visualization, Fig. 8 shows these three global mechanisms and experimental data results.

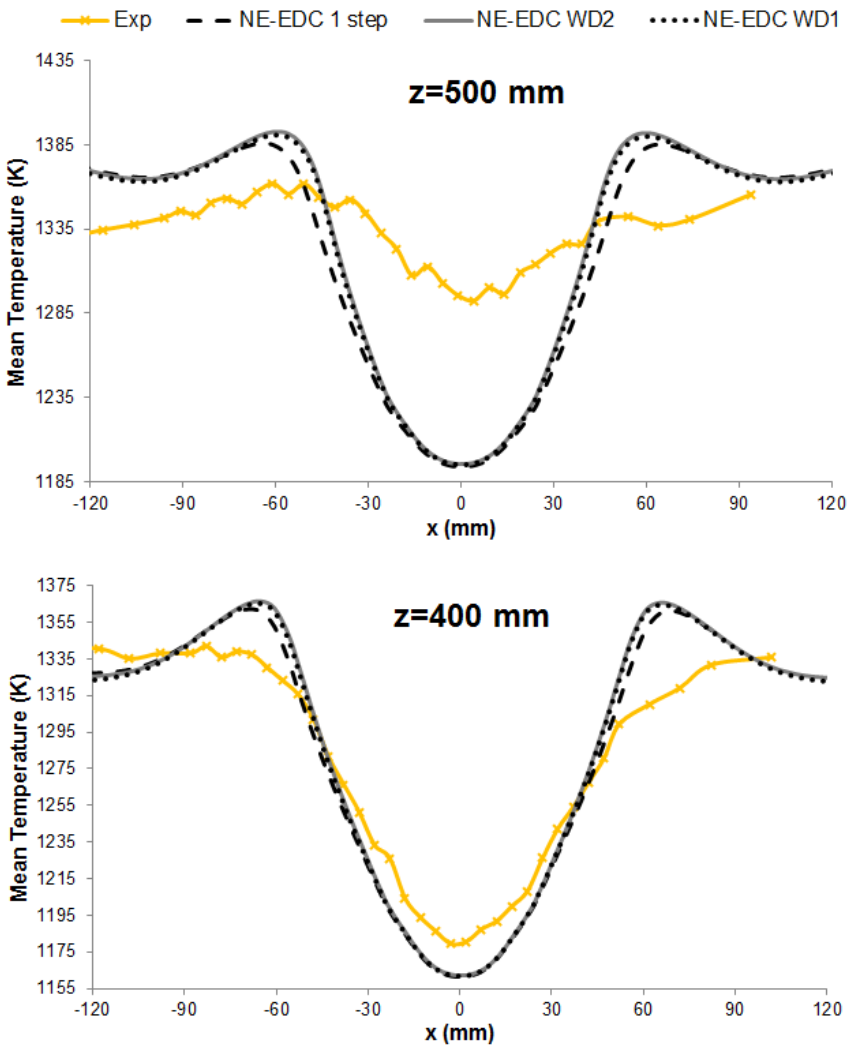

Fig. 8 *Comparison of mean temperature from experimental measurements and from NE-EDC –step, NE-EDC WD1 and NE-EDC WD2.*

It can be appreciated that the WD1 and WD2 modelling results are almost the same. Thus, it can be concluded that the CO oxidation rates do not have a huge impact over the mean temperature

in this case. At this point, it should be noted that, during the modelling, it took more time to converge the WD1 model than the WD2 model, so that with the results of both models being similar, WD2 is recommended from a modelling point of view. The convergence difference between WD1 and WD2 can be related to the β coefficient value, which is not equal to 0 for the WD2 case. The CPU time for each global mechanism with a 2 core CPU@ 2.5 GHz is displayed in Table 3. It should be clarified that the displayed computational time is starting from a convergence reacting flow-field of the NE-EDC model with 1-step reaction mechanism for chemical time calculation:

Table 3 *CPU computational time*

	Computational time	**Convergence of temperature**
JL1	23 h	Straight line
WD1	148 h	Sine wave
WD2	22 h	Straight line

Between the 1-step global mechanism and the WD2, a slight difference can be appreciated at z=400 mm and z=500 mm heights. Close to the furnace centre (|x| < 60 mm), the WD2 underpredicts the mean temperature less than the 1-step mechanism at both heights. For example, at |x|=36 mm, the deviation of the WD2 model is 3.5%, while the 1-step mechanism provides a deviation of 5.5%. Therefore, the WD2 slightly improves flameless combustion modelling in combination with the NE-EDC model constant calculation idea.

In order to analyse if modelling results can be affected by the use of a more extended chemical mechanism to calculate temperature and species concentrations during modelling, another modelling have being repeated by the use of the GRI 3.0 mechanism (53 species) [40]. As it is shown in Fig. 9 no difference it is appreciated between the use of Smooke (16 species) and GRI 3.0 (53 species) detail mechanisms for mean temperature predictions.

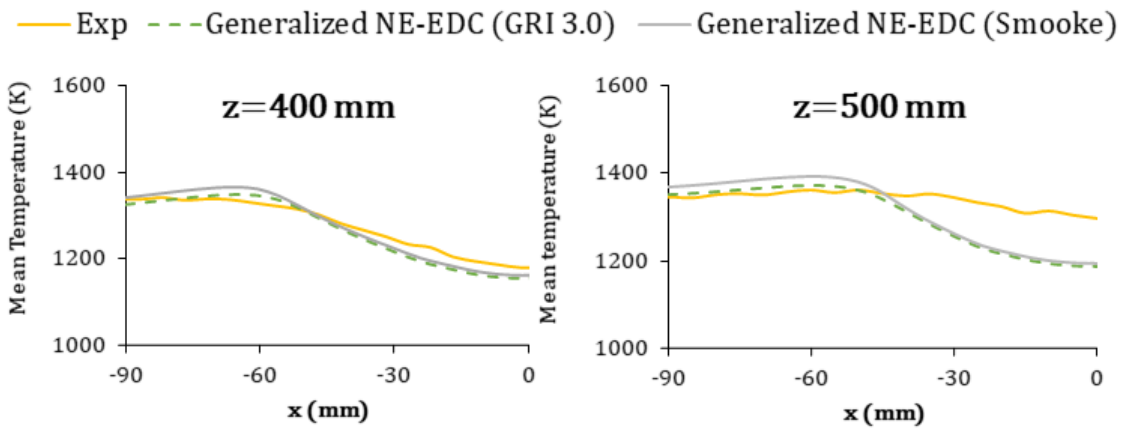

Fig. 9 *Comparison of mean temperature from experimental measurements and from Generalized NE-EDC (with WD2 global mechanism in combination with Smooke and GRI 3.0 detail chemistry*

Although the WD2 global mechanism has slight improvements, it does not seem that taking into account CH_4, H_2, O_2, CO and CO_2 species in the chemical time scale calculation notably affects the results of the model. This suggests little interaction between reaction zones for this application. The interaction between the reaction zones has more effect on mean temperature predictions in the JHC burner [21] than in the enclosed furnace. This could be related to the findings of Xu's experimental data [41], where the stabilized flames in JHC flames did not appear in the main reaction zone of the Delft lab-scale furnace. This could be due to the dynamic mixing in the Delft lab-scale furnace, where the recirculation of the internal flue gases stretches the flame front. As future work, more case studies should be needed to verify the improvements offered by the Generalized NE-EDC studied here.

In any case, the NE-EDC model, in combination with the WD2, called here the Generalized NE-EDC model, gives better predictions of the radial profiles of the mean temperature as compared to the 1-step global mechanism. For this reason, WD2 is selected as the best global mechanism model to consider the interaction between the reaction zones during flameless modelling, without too much impact on computational time.

5 Conclusion

In this work, the NE-EDC model is updated by calculating the chemical time scale while also considering minor species, such as, CH_4, H_2, O_2, CO and CO_2, called here the Generalized NE-EDC model. This improvement is interesting to analyse, considering the latest conclusions taken

from the DNS modelling results, where it is suggested that interactions between the reaction zones influence the behaviour of the temperature field and reaction zone.

The detailed methodology presented in this work aims to improve the chemical time scale calculation τ_c by a simple generalized method, in combination with the NE-EDC model; while not increasing the computational time during modelling. Therefore, global reaction mechanisms adjusted for flameless combustion are suggested for its use.

A comparative study of four global reaction mechanisms is carried out in combination with the NE-EDC model to model the Delft lab-scale furnace and results are compared against those experimental measurements. The differences in the modelling results start to be appreciated above a height of 200 mm as, according to experimental data, the reaction rate influence on the mean temperature profile starts at a height of 200 mm. Although the JL1 model provides good results in other works [26]-[27], in this specific application, close to the top wall of the furnace, the mean temperature is overpredicted, moving away from experimental data. The WD1 mechanism provided similar results to the WD2 mechanism, but from a numerical point of view, the numerical convergence of WD1 takes 6 times longer before convergence occurs. The convergence difference can be related to the β coefficient value, which is not equal to 0 for the WD2 case. Therefore, it was found that the WD2 is the best model, as it underpredicts the mean temperature close to the centre of the furnace ($|x| < 60$ mm) at z=400 and z=500 mm by less. Nevertheless, the 1-step global mechanism is also a good choice.

Although, in this application, the WD2 provides slight improvements, the realistic chemical time scale calculation methodology applied in this work does not notably affect the results of the model. This suggests little interaction between reaction zones in the context of the NE-EDC model and is based on a set of relatively small mechanisms. It was shown that the interaction between the reaction zones has more effect on the mean temperature predictions in the JHC burner [21]. In this work, an enclosed furnace is analysed where, according to experimental data, the stabilized flames seen in the JHC flames did not appear in the main reaction zone of the Delft lab-scale furnace. This could be due to the dynamic mixing in the Delft lab-scale furnace, where the recirculation of the internal flue gases stretches the flame front, so that the interaction between reaction zones can be lower.

Here, the WD2 in combination with the NE-EDC model's constant calculation methodology, called here Generalized NE-EDC, gives a more accurate prediction of the radial profiles of the mean temperature, especially where the autoignition is more frequent. However, for this specific application, the interactions between the reaction zones do not have too much impact on the mean temperature prediction.

Acknowledgements

We would like to thank Professor Dirk Roekaerts at TU Delft (the Netherlands) for his courtesy in sharing with us the experimental data of the Delft lab-scale furnace.

Declaration of competing interest

The authors declare that they have no known competing financial interests or personal relationships that could have appeared to influence the work reported in this paper.

Funding

This research did not receive any specific grant from funding agencies in the public, commercial, or not-for-profit sectors.

CRediT authorship contribution statement

N. Romero-Anton: Conceptualization, Methodology, Software, Validation, Visualization, Writing – original draft**. K. Martin-Eskudero:** Conceptualization, Supervision, Writing – original draft. **Memgmeng Ran**: Conceptualization, Formal analysis. **Z. Azkorra Larrinaga:** Supervision, Writing – review & editing.

References

[1] Wünning, J.A., Wünning, J.G.: Flameless oxidation to reduce thermal NO-formation. Prog. Energy Combust. Sci. 23, 81-94 (1997)

[2] Cavaliere, A., de Joannon, M. : Mild combustion. Prog. Energy Combust. Sci. 30, 329-366 (2004)

[3] Dally, B.B., Karpetis, A.N., Barlow, R.S.: Structured of turbulent non-premixed jet flames in a diluted hot flow. Combust. Flame 27, 2255-2265 (2002)

[4] Oldenhof, E., Tummers, M.J., van-Veen, E.H., Roekaerts, D.J.E.M.: Conditional flow field statistics of jet-in-hot-coflow flames. Combust. Flame 160, 1428-1440 (2013)

[5] Cavigiolo, A., Galbiati, M.A., Effuggi, A., Gelosa, D., Rota, R.: Mild combustion in a laboratory-scale apparatus. Combust. Sci. Technol. 175, 1347-1367 (2003)

[6] Rebola, A., Costa, M., Coelho, P.J.: Experimental evaluation of the performance of a flameless combustor. Appl. Therm. Eng. 50, 805-815 (2013)

[7] Perpignan, A.A.V., Gangoli-Rao, A., Roekaerts, D.J.E.M.: Flameless combustion and its potential towards gas turbines. Prog. Energy Combust. Sci. 69, 28-62 (2018)

[8] Ren, M., Wang, S., Romero-Anton, N., Zhao, J., Zou, C., Roekaerts, D.: Numerical study of a turbulent co-axial non-premixed flame for methanol hydrothermal combustion: comparison of the EDC and FGM models. J. Supercrit. Fluids 169, 105132 (2020)

[9] Rehm, M., Seifert, P., Meyer, B.: Theoretical and numerical investigation on the EDC-model for turbulence–chemistry interaction at gasification conditions. Comput. Chem. Eng. 33, 402-407 (2009)

[10] Graça, M., Duarte, A., Coelho, P.J., Costa, M.: Numerical simulation of a reversed flow small-scale combustor. Fuel Proc. Technol. 107, 126-137 (2013)

[11] Parente, A., Malik, M.R., Contino, F., Cuoci, A., Dally, B.B.: Extension of the Eddy Dissipation Concept for turbulence/chemistry interactions to MILD combustion. Fuel 63, 98-111 (2016)

[12] Romero-Anton, N., Huang, X., Bao, H., Martin-Escudero, K., Salazar-Herran, E., Roekaerts, D.: New extended eddy dissipation concept model for flameless combustion in furnaces. Combust. Flame 220, 49-62 (2020)

[13] Lewandowski, M.T., Ertesvåg, I.S.: Analysis of the Eddy Dissipation Concept formulation for MILD combustion modelling. Fuel 224, 687-700 (2018)

[14] Ertesvåg, I.S.: Analysis of Some Recently Proposed Modifications to the Eddy Dissipation Concept (EDC). Combust. Sci. Technol. 192, 1-29 (2019)

[15] Magnussen, B.F., Hjertager, B.: On the structure of turbulence and a generalized eddy dissipation concept for chemical reaction in turbulent flow. 19th AIAA Aerospace Meeting, St. Louis (1981).

[16] Magnussen, B.F.: The eddy dissipation concept a bridge between science and technology. ECCOMAS thematic conference on computational combustion, Lisbon, Portugal (2005)

[17] Minamoto, Y., Dunstan, T.D., Swaminathan, N., Cant, R.S.: DNS of EGR-type turbulent flame in MILD condition. Proc. Combust. Inst. 34, 3231-3238 (2013)

[18] Minamoto, Y., Swaminathan, N.: Modelling paradigms for MILD combustion. Int. J. Adv. Eng. Sci. Appl. Math 6, 65-75 (2014)

[19] Minamoto, Y., Swaminathan, N.: Scalar gradient behaviour in MILD combustion. Combust. Flame 161, 1063-1075 (2004)

[20] Swaminathan, N.: Physical Insights on MILD Combustion From DNS. Frontiers in Mechanical Engineering 5 (2019)

[21] Evans, M.J., Petre, C., Medwell, P.R., Parente, A.: Generalisation of the eddy-dissipation concept for jet flames with low turbulence and low Damköhler number. Proc. Combust. Inst. 37, 4497-4505 (2019)

[22] Lewandowski, M. T., Parente, A., & Pozorski, J.: Generalised Eddy Dissipation Concept for MILD combustion regime at low local Reynolds and Damköhler numbers. Part 1: Model framework development. Fuel, 278, 117743 (2020)

[23] Lewandowski, M. T., Li, Z., Parente, A., & Pozorski, J.: Generalised Eddy Dissipation Concept for MILD combustion regime at low local Reynolds and Damköhler numbers. Part 2: Validation of the model. Fuel, 278, 117773 (2020).

[24] Driscoll, J.F., Chen, J.H., Skiba, A.W., Carter, C.D., Hawkes, E.R., Wang, H.: Premixed flames subjected to extreme turbulence: Some questions and recent answers. Prog. Energy Combust. Sci. 76, 100802 (2020)

[25] Minamoto, Y., Swaminathan, N., Cant, S.R., Leung, T.: Morphological and statistical features of reaction zones in MILD and premixed combustion. Comb Flame 161, 2801-2814 (2014)

[26] Kim, J.P., Schnell, U., Scheffknecht, G.: Comparison of different global reaction mechanisms for MILD combustion of natural gas. Combust. Sci. Technol. 180, 565-592 (2008)

[27] Wang L, Liu Z, Chen S, Zheng C.: Comparison of Different Global Combustion Mechanisms Under Hot and Diluted Oxidation Conditions. Combust. Sci. Technol. 184, 259-276 (2012)

[28] Bösenhofer, M., Wartha, E. M., Jordan, C., Harasek, M.: The eddy dissipation Concept—Analysis of different fine structure treatments for classical combustion. Energies 11, 1902 (2018)

[29] Galletti, C., Parente, A., Tognotti, L.: Numerical and experimental investigation of a mild combustion burner. Combust. Flame 151, 649-664 (2007)

[30] Jones, W.P., Lindstedt, R.P.: Global reaction schemes for hydrocarbon combustion. Combust. Flame 73, 233 (1988)

[31] Westbrook, C.K., Dryer, F.L.: Chemical Kinetic Modeling of Hydrocarbon Combustion. Prog. Energy Combust. Sci. 10, 1-57 (1984)

[32] Peters, N.: Numerical and asymptotic analysis of systematically reduced reaction schemes for hydrocarbon flames, Numerical simulation of combustion phenomena. Springer, Heidelberg (1985)

[33] Peters, N., Williams, F.A.: The Asymptotic Structure of Stoichiometric Methane-Air Flames. Combust. Flame 68, 185-207 (1987)

[34] Smoke, M.D., Giovangigli, V.: Formulation of the premixed and nonpremixed test problems. In: Reduced kinetic mechanisms and asymptotic approximations for methane-air flames. pp. 1-28. Springer, Heidelberg (1991)

[35] Marinov, N.M., Westbrook, C.K., Pitz, W.J.: Detailed and global chemical kinetics model for hydrogen. In: Chan, S.H. (eds) Transport Phenomena in Combustion, pp.118-129. Taylor & Francis, Washington (1996)

[36] Andersen, J., Rusmussen, C.L., Giselsson, T., Glarborg, P.: Global combustion mechanisms for use in CFD modeling under oxy-fuel conditions. Energy Fuels 23, 1379-1389 (2009)

[37] Poinsot, T., Veynante, D.: Theoretical and numerical combustion. RT Edwards (2005)

[38] Fox, R.O.: Computational Models for turbulent Reacting Flows. Cambridge, UK (2003)

[39] Wartha, E.M., Bösenhofer, M., Harasek, M.: Characteristic Chemical Time Scales for Reactive Flow Modeling. Combust. Sci. Technol. (2020).

[40] Smith, G. P., Golden, D. M., Frenklach, M., Moriarty, N. W., Eiteneer, B., Goldenberg, M., Bowman, C. T., Hanson, R. K., Song S., Gardiner, W. C., Lissianski, V. V., Qin, Z., GRI-mech 3.0. Retrieved from http://combustion.berkeley.edu/gri-mech/version30/text30.html (2020). Accessed June 2020

[41] Huang, X.: Measurements and Model Development for Flameless Combustion in a lab-scale furnace. Ph. D. Thesis, Delft University of Technology (2018).